Acoustic Emission-Based Detection in Restricted-Access Areas Using Multiple PZT Disc Sensors

Lu Cheng[1](✉), Ali Nokhbatolfoghahai[2], Roger M. Groves[2], and Milan Veljkovic[1]

[1] Faculty of Civil Engineering and Geosciences, Delft University of Technology, Delft, The Netherlands
l.cheng-2@tudelft.nl

[2] Faculty of Aerospace Engineering, Delft University of Technology, Delft, The Netherlands

Abstract. The performance of the Acoustic Emission (AE) technique is significantly dependent on the sensors attached to the structural surface. Although conventional commercially AE sensors, like R15a and WSa sensors, have been extensively employed in monitoring many different structures, they are unavailable in restricted-assess areas. In contrast, thin PZT sensors are small, inexpensive and lightweight. These thin PZT sensors have a great potential for passive sensing to detect AE signals. However, their utility in AE monitoring is limited due to their low signal-to-noise ratio and information incompleteness because of their simple construction. This work discusses the issues and possible solutions with regards to the specific selection and application of thin PZT sensors for passive sensing. The compatibility of different thin PZT sensors and conventional bulky sensors is investigated using pencil break lead (PBL) tests. The comparison between the recorded signals is carried out in both the time domain and frequency domain for these sensors. To improve the reliability and performance of the thin PZT sensors, a methodology employing multiple thin PZT sensors of different sizes is proposed based on machine learning techniques and sensor data fusion.

Keywords: Acoustic emission technique · Thin PZT sensors · Restricted-assess areas · Data fusion · Machine learning

1 Introduction

Acoustic emission (AE) technology plays a crucial role in structural health monitoring (SHM) as a non-destructive testing method [1]. A typical AE system consists of a network of sensors and preamplifiers. As shown in Fig. 1, the AE sensors are located at the surface of the structure to transmit the surface motion *f(t)* from the elastic waves into electrical signals *a(t)*. Mathematically, the input function *f(t)* of the surface motion is transformed into the function *a(t)* of electrical signals sequentially by transfer functions of the AE sensors *w(t)*, filter $w_f(t)$, amplifier $w_a(t)$. These recorded signals can then be analyzed to extract valuable information about the nature of the source of emission. In general, the frequency response of both $w_f(t)$ and $w_a(t)$ are known to be fairly flat or almost linear in the frequency domain [2]. Thus, AE sensors are the heart of the AE instrument.

P. Rizzo and A. Milazzo (Eds.): EWSHM 2022, LNCE 253, pp. 619–629, 2023.
https://doi.org/10.1007/978-3-031-07254-3_62

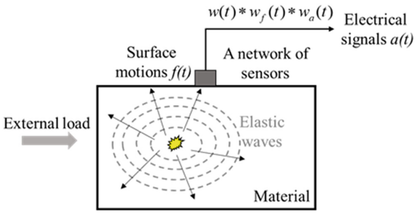

Fig. 1. Acoustic emission (AE) principle

Compared to other piezoelectric materials, PZT (Lead Zirconate Titanate) is the most widely used material to fabricate AE sensors. Conventional AE sensors are normally made of bulky piezoelectric ceramics sandwiched between electrodes and backing materials as illustrated in Fig. 2. These sensors are enclosed in a protective metal housing to minimize interference and enhance the sensitivity of the response. Conventional bulky AE sensors, such as R15α and WSα transducers, have been extensively employed in many different structures [3]. However, the implementation of these bulk sensors is limited in restricted-access areas of interest. A general trend in employing thin PZT sensors of several millimeters height has been observed toward overcoming this space limitation.

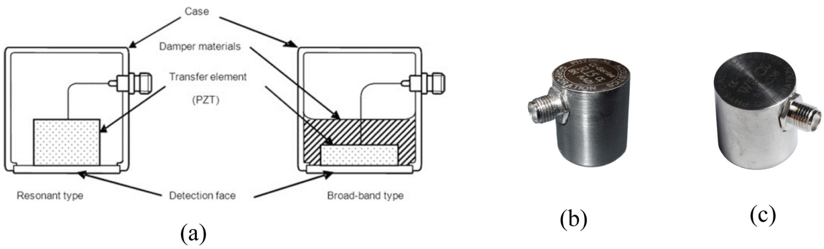

Fig. 2. (a) Conventional PZT bulky AE sensor [4]; (b) R15α sensor; (c) WSα sensor

Thin PZT sensors are well known for their dual application as either actuators or sensors [5]. Thin PZT sensors have been commonly employed for ultrasonic guided wave excitation and detection in the fields of SHM. Compared to commercial AE sensors, thin PZT sensors are small, inexpensive and lightweight with a broadband frequency response. In the past few years, many researchers have investigated the feasibility of thin PZT sensors for monitoring acoustic emission activity. Studies have demonstrated the great potential of thin PZT sensors for passive sensing in the field of AE monitoring in plate-like metallic structures [6]. However, thin PZT sensors suffer from the issues of a less favorable signal-to-noise ratio compared to conventional AE sensors [7]. Besides, the comparison of thin PZT sensors with conventional AE sensors in previous studies have been confined to thin PZT sensors with a certain geometry and no selection methodology has been proposed to select appropriate thin PZT sensors for passive sensing. A more detailed analysis and comparison between thin PZT sensors and conventional bulky AE transducers is still required. Meanwhile, several studies have shown the limitations of using one type of PZT sensor in AE identification [8]. It can only collect partial information and therefore cannot extract precise features about the damage. This necessitates improving the reliability of AE monitoring with a careful design configuration of multiple thin PZT sensors.

The main objective of this study is to propose a possible solution to improve the application of thin PZT sensors for passive sensing. Criteria for application-specific selection of the thin PZT disc sensors are proposed to improve the performance using multiple sensors. A comparative study between the thin PZT sensors and two commercial AE sensors, which are consolidated in the academic and industrial community, is carried out in this study. Pencil break lead (PBL) tests are performed on a compact tension specimen. Additionally, an advanced signal processing method based on machine learning approaches and sensor data fusion is proposed to improve the reliability of the AE monitoring using thin PZT sensors.

2 Thin PZT Sensors

2.1 Theoretical Background

A customized version of thin PZT sensors can be easily made and ordered according to the specific application. Several key parameters should be taken into account for selecting thin PZT sensors, such as shape, material and geometry. In contrast to PZT sensors of non-circular shape, a circular one receives signals evenly from all directions and is more often used in practical cases. One of the most significant material properties of PZT for passive sensing application [5] is the piezoelectric voltage coefficient g_{31}, which should be maximized.

The sensor response as a function of frequency has been the subject of many studies over the years [9]. The specific frequency response of conventional bulky AE sensors can be obtained from the manufacturer, however is not available for thin PZT sensors. Ochôa et al. proposed using this formulation for the sensor output voltage V_0 including the influence of sensor radius and frequency:

$$|V_0| \propto \left| r_a \left[\sum_{\xi^S} \xi^S J_1(\xi^S r_a) + \sum_{\xi^A} \xi^A J_1(\xi^A r_a) \right] \right| = f(\xi^S, \xi^A, r_a) \tag{1}$$

where r_a is the sensor radius, ξ^S and ξ^A are the wavenumbers of the symmetric and antisymmetric Lamb wave modes, respectively, and J_1 is the Bessel function of Order 1. The frequency sensitivity of thin PZT sensors as receivers under different radius can be evaluated using Eq. (1).

Due to the electro-mechanical (E/M) behavior, the piezo ceramic may experience two extreme states, resonance and anti-resonance. Typically, an unstable transitory regime can be formulated from the points of resonance and anti-resonance. This regime is detrimental for the steady and reliable application of PZT sensors, which should be avoided. Giurgiutiu [10] proposed equations to calculate the admittance $Y(w)$ and impedance $Z(w)$ of circular PZT sensors constrained by a structure:

$$Y(w) = iw\overline{C}\left\{1 - k_p^2\left[1 - \frac{(1+v_a)J_1(\overline{\phi})}{\overline{\phi}J_0(\overline{\phi}) - [(1-v_a) - \overline{\chi}(w)(1+v_a)]J_1(\overline{\phi})}\right]\right\} \tag{2}$$

$$Z(w) = Y^{-1}(w) = \frac{1}{iw\overline{C}}\left\{1 - k_p^2\left[1 - \frac{(1+v_a)J_1(\overline{\phi})}{\overline{\phi}J_0(\overline{\phi}) - [(1-v_a) - \overline{\chi}(w)(1+v_a)]J_1(\overline{\phi})}\right]\right\}^{-1} \quad (3)$$

The detailed calculation of the above unknown parameters can be found in [10]. The zeros of the denominator of Eq. (2) represent the resonance points, whereas the anti-resonance points correspond to the zeros of the entire expression inside the curly brackets of Eq. (2). The sensor thickness is considered in the E/M response, which allows the selection of the appropriate thickness for thin PZT sensors.

2.2 Criteria for Sensor Selection

Ochôa [11] provided a comprehensive discussion about the design methodology for both actuating and sensing application of thin PZT disc. However, in the AE application, the only purpose of using thin PZT sensors is for sensing. The criteria adopted in this research is summarized below:

a) The sensors should have enough sensitivity in the frequency range for the specific application with a high piezoelectric voltage coefficient g_{31};
b) The local maximum in the sensor output function should not overlap with or be close to the E/M resonance or anti-resonance of the bonded thin PZT sensors.
c) A thicker PZT sensor is favored, as the amplitude of sensor output response is directly proportional to the thickness.

3 Experimental Setup

3.1 Selected Sensors for Measurements

According to the selection methodology described in Sect. 2, three types of thin PZT sensors were selected for analysis. The procedure can be described as following steps: (1) Calculate the sensor output function of thin PZT sensors with different diameters using Eq. (1); (2) Select several types of thin PZT sensors which have enough sensitivity in the frequency range of interest for the application; (3) To consider the sensor thickness, the E/M response for selected thin PZT sensors with different thickness (<1 mm) are calculated according to Eq. (2); Select the alternative thickness satisfying criteria b). (4) Choose the larger thickness to get higher sensitivity. The properties of the sensors analysed are illustrated in Fig. 3 and Table 1.

Figure 4 shows the frequency sensitivity response of the R15α sensor and WSα sensor. The sensor output function in different scales of the selected thin PZT sensors is shown in Fig. 5 according to Eq. (1). The frequency range for metallic structures is recommended as 100 kHz–900 kHz [15]. Considering that the attenuation of signals increases with frequency, frequencies above 500 kHz are meaningless for most applications and are cut-off to minimize electronic noise. In Fig. 5 (b), the sensor output voltage is converted to decibels using dB = 20 $\log_{10}$(y). It can be observed that these three thin PZT sensors could together cover the frequency range, which cannot be achieved

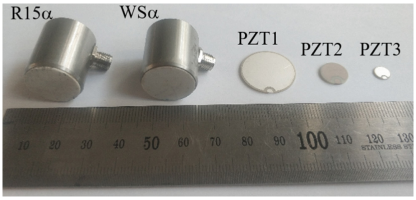

Fig. 3. Illustration of the applied sensor in the measurement

Table 1. Dimensions and properties of selected sensors

	R15α	WSα	PZT-1	PZT-2	PZT-3
Radius (mm)	9.5	9.5	10	5	3
Thickness (mm)	22.4	21.4	0.79	0.8	0.5
Material	PZT-5A [12]	PZT-5A	PIC155	PIC155	PIC255
$g_{31} \times 10^{-3}$ (Vm/N)	−12.4	−12.4	−12.9	−12.9	−11.3
Weight (g)	34	32	1.9	0.49	0.18

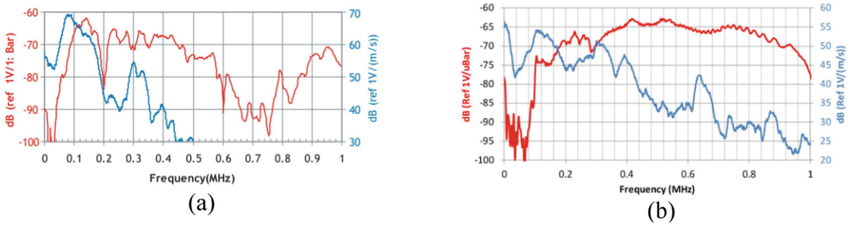

Fig. 4. Sensitivity response of (a) R15α sensor [13]; (b) WSα sensor [14]

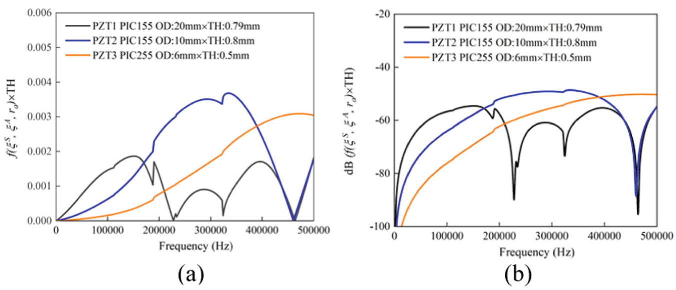

Fig. 5. Sensor output voltage of selected thin PZT sensors in different scale

by individual thin PZT sensors. The sensor output function and E/M response of the selected thin PZT sensors are shown in Fig. 6. There are two E/M resonances for PZT-1 and one for PZT-2 between 0 and 500 kHz. All the relevant sensor local maximum are away from the E/M resonances, as seen from Fig. 6.

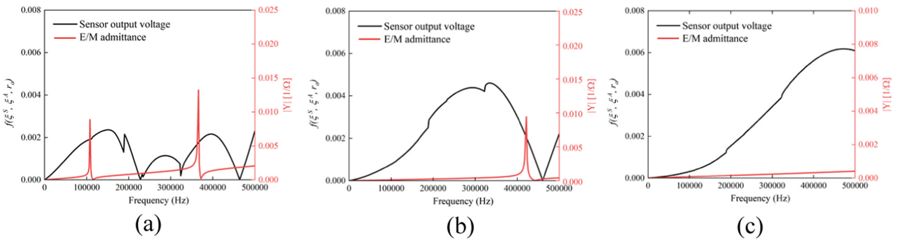

Fig. 6. Sensor output function and Electro-mechanical admittance response of selected thin PZT sensors: (a) PZT-1, (b) PZT-2 and (c) PZT-3

3.2 Measurement Set-Up

PBL tests are performed on a compact tension (CT) specimen made of S355 steel with the dimensions 85 mm × 85 mm × 15 mm. To eliminate vibrations and energy transmission from the environment into the specimen, the CT specimen was supported on a polymer foam as shown in Fig. 7. Two different experimental set-ups were used with different sensor combinations, as seen from Fig. 8: (a) R15α and three thin PZT sensors; and (b) WSα and three thin PZT sensors. During testing, the pencil lead is broken at the notch tip of the CT specimen to simulate real crack initiation at a distance of 30 mm from each sensor. An eight-channel MISTRAS AEwin data acquisition system (Physical Acoustic Corporation Micro-II) with a sampling rate of 5MSPS and a 40 dB PAC 2/4/6 pre-amplification was used. Ambient noise was filtered using a threshold of 50 dB.

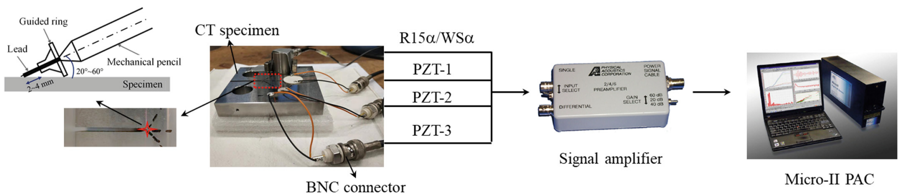

Fig. 7. Experimental set-up

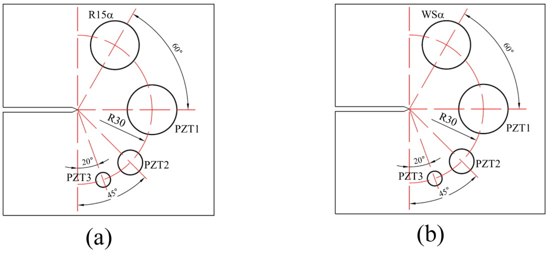

Fig. 8. Layout of sensors for the different combinations: (a) R15α and three thin PZT sensors; and (b) WSα and three thin PZT sensors.

4 Results and Discussion

Figure 9 presents the response of signals in the time domain and frequency domain from pencil breaking. Significant differences in the waveforms can be recognized. It can be seen that only PZT-3 shows a typical burst shape under the excitation, while other sensors present mixed signals containing both burst and continuous types. Signals received by sensors with a larger size are significantly distorted as a result of the aperture effect, increasing the possible distortion due to scattering or reflections [16], requiring improvements in the detection accuracy by post-processing techniques. Differences are also strong in the frequency spectra using Fast Fourier Transform (FFT) of the waveforms as well, as seen in Fig. 9 (b), (d), (f), (h) and (j). The partial power feature can provide a more reliable description of AE signals. It can be calculated by summing the power spectrum in a user-defined range of frequencies, dividing it by the total power.

$$PP_{(f_1:f_2)} = \int_{f_1}^{f_2} \widetilde{U}^2(f)df \Big/ \int_0^{2500\text{kHz}} \widetilde{U}^2(f)df \quad (4)$$

where $\widetilde{U}(f)$ is the power spectral density using fast Fourier Transformation of the signals. The average value of $PP_{(80:500\ \text{kHz})}$ is obtained as 92% from WSα sensor. A flat frequency response and wideband range of WSα sensor allow identifying the predominant frequency band of AE sources.

The characteristics of the signals recorded from different sensors are described in Table 2. The WSα sensors clarify that the nature of the frequency content of the signal source is within 200–400 kHz, while the frequency content of the signal source is changed significantly to 80–200 kHz using the R15α sensor. It is reported that the thin PZT sensors are non-resonant devices with wide frequency-band capabilities [17]. However, the last column of Table 2 presents that the original frequency content of the signal source is also altered due to the frequency response of thin PZT sensors. The results emphasize the limitation of using only one type of thin PZT sensor.

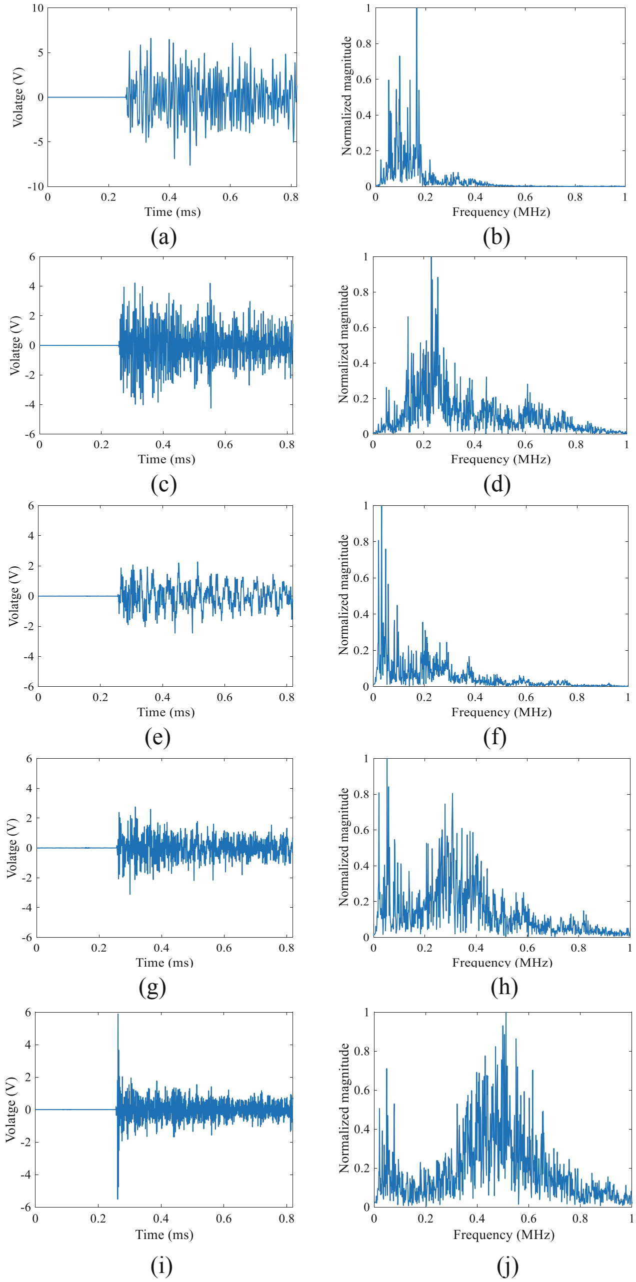

Fig. 9. Example waveforms and corresponding frequency spectra of signals captured by R15α (a) and (b), WSα (c) and (d), PZT-1 (e) and (f), PZT-2 (g) and (h), PZT-3 (i) and (j).

Table 2. Characteristics of signals received from different sensors

	Amplitude (dB)	Resonant frequency of sensor (kHz)	Frequency band with high sensitivity (kHz)
R15α	99	150	80–200
WSα	93	650	200–400
PZT-1	96	150/284/396	170–320
PZT-2	92	330	250–450
PZT-3	94	470	300–600

5 Proposed Technology Using Multiple Thin PZT Sensors

Normally, AE features from different types of sensors cannot be compared as the sensitivity responses between sensors are different. Data fusion is an approach for the integration of various types of data to generate more information from the combined data than from interpreting each dataset individually. Within the recent few years, deep learning-based approaches for data fusion received extensive attention across various research fields due to the enhancement of computing capability. Considering the favourable signal-to-noise ratio of conventional bulky sensors, a method is proposed to reconstruct the signals of conventional AE sensors by using the signals from multiple thin PZT sensors. As shown in Fig. 10, the signals from selected thin PZT sensors can be stored in an image file as the input data of the deep convolution neural network. The output data is the waveform from conventional bulky sensors. Then, the features can be extracted from the reconstructed signals for further damage detection. The development of this model is the current work in progress.

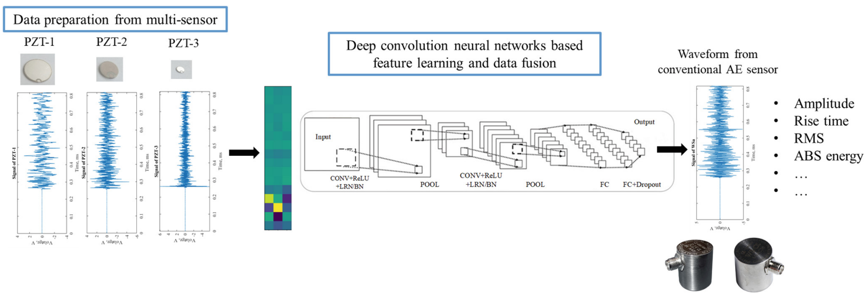

Fig. 10. Flowchart illustrating of the proposed method

6 Conclusions

1. In terms of the passive application of thin PZT sensors, the criteria for defining the suitable sensors are recommended considering the voltage output and E/M response within the interest frequency band.

2. Compared to thin PZT sensors, R15α shows the benefit of sensitivity with much higher amplitude, while WSα generates the most faithful representation of the nature of the AE source in a wider frequency band. Thin PZT sensors capture signals with an altered frequency content of the signal and a smaller amplitude compared to R15α sensors.
3. To improve the performance of multiple thin PZT sensors for passive sensing, a possible solution of using a deep neural network to reconstruct the signals from conventional bulky sensors is proposed. The performance of the proposed method will be evaluated in the future.

Acknowledgement. The first author wishes to express her gratitude to the financial support of CSC Scholarship Council under grant number 201806060122. Dr. Ali Nokhbatolfoghahai is supported by the AIRTuB project (Automatic Inspection and Repair of Turbine Blades), funded with a Top Sector Energy subsidy from the Ministry of Economic Affairs of the Netherlands.

References

1. He, Y., et al.: An overview of acoustic emission inspection and monitoring technology in the key components of renewable energy systems. Mech. Syst. Sig. Process. **148**, 107146 (2021)
2. Grosse, C.U., Ohtsu, M.: Acoustic Emission Testing. Springer, Heidelberg (2008). https://doi.org/10.1007/978-3-540-69972-9
3. Cheng, L., Xin, H., Groves, R.M., Veljkovic, M.: Acoustic emission source location using Lamb wave propagation simulation and artificial neural network for I-shaped steel girder. Constr. Build. Mater. **273**, 121706 (2021)
4. The Japanese Society for Non-Destructive Inspection: Practical Acoustic Emission Testing. Springer, Japan (2016). https://doi.org/10.1007/978-4-431-55072-3
5. Giurgiutiu, V., Zagrai, A.N.: Characterization of piezoelectric wafer active sensors. J. Intell. Mater. Syst. Struct. **11**(12), 959–976 (2001)
6. Yu, L., Momeni, S., Godinez, V., Giurgiutiu, V., Ziehl, P., Yu, J.: Dual mode sensing with low-profile piezoelectric thin wafer sensors for steel bridge crack detection and diagnosis. Adv. Civ. Eng. **2012** (2012)
7. Trujillo, B., Zagrai, A., Meisner, D., Momeni, S.: Monitoring of acoustic emission activity using thin wafer piezoelectric sensors. In: Proceedings of the SPIE 9064, Health Monitoring of Structural and Biological Systems (2014)
8. Hamam, Z., Godin, N., Fusco, C., Monnier, T.: Modelling of acoustic emission signals due to fiber break in a model composite carbon/epoxy: experimental validation and parametric study. Appl. Sci. **9**(23), 1–24 (2019)
9. Ono, K., Cho, H., Vallen, H., M'Closkey, R.T.: Transmission sensitivities of contact ultrasonic transducers and their applications. Sensors **21**(13), 4396 (2021)
10. Ochôa, P., Groves, R.M., Benedictus, R.: Systematic multiparameter design methodology for an ultrasonic health monitoring system for full-scale composite aircraft primary structures. Struct. Control Health Monit. **26**(5), e2340 (2019)
11. Giurgiutiu, V.: Structural Health Monitoring with Piezoelectric Wafer Active Sensors. Elsevier (2007)
12. Boukabache, H., Escriba, C., Fourniols, J.-Y.: Toward smart aerospace structures: design of a piezoelectric sensor and its analog interface for flaw detection. Sensors **14**(11), 20543–20561 (2014)

13. Model_R15a. https://www.physicalacoustics.com/content/literature/sensors/Model_R15a.pdf. Accessed 20 Feb 2020
14. Model_WSa. https://www.physicalacoustics.com/content/literature/sensors/Model_WSa.pdf. Accessed 20 Feb 2020
15. Ozevin, D.: MEMS acoustic emission sensors. Appl. Sci. **10**(24), 1–14 (2020)
16. Tsangouri, E., Aggelis, D.G.: The influence of sensor size on acoustic emission waveforms—A numerical study. Appl. Sci. **8**(2), 168 (2018)
17. Giurgiutiu, V., Zagrai, A., Jing Bao, J.: Piezoelectric wafer embedded active sensors for aging aircraft structural health monitoring. Struct. Health Monit. **1**(1), 41–61 (2002)